J Nanopart Res (2011) 13:3275–3286
DOI 10.1007/s11051-011-0242-1

RESEARCH PAPER

Organic-phase synthesis of self-assembled gold nanosheets

TamilSelvi Selvam · Chao-Ming Chiang · Kai-Ming Chi

Received: 16 September 2010 / Accepted: 17 January 2011 / Published online: 30 January 2011

Abstract Amphiphilic gold nanoclusters with the diameter of 1.8 ± 0.2 nm were prepared by decomposition of organometallic gold precursor CH_3Au-PPh_3 in the presence of mercaptoacids in *o*-xylene. Self-assembly of the 16-mercaptohexadecanoic acid protected gold clusters led to the formation of the nanosheets consisted of aligned gold clusters. The hydrogen bonding between the carboxylic groups attached on the adjacent gold clusters likely drives the self-assembly. This phenomenon was cross-verified by employing the preheated mercaptoacid-amine surfactant system where a part of the mercaptoacids and amines were converted into $–NH_3^+–^-OOC–$ ion pair and interrupting a part of the hydrogen bonding sites to lead to the reduction in the size of the structures from nanosheets to nanobelts. Interestingly, we found the dependency of the luminescent properties on the extent of maintaining the self-assembly of the clusters intern dictated by the surfactants.

Keywords Organic-phase synthesis · Self-assembly · Amphiphilic gold nanosheets · Luminescent gold nanoclusters

Electronic supplementary material The online version of this article (doi:10.1007/s11051-011-0242-1) contains supplementary material, which is available to authorized users.

T. Selvam · K.-M. Chi (✉)
Department of Chemistry and Biochemistry, National Chung Cheng University, Min-Hsiung, Chia-Yi 621, Taiwan
e-mail: chekmc@ccu.edu.tw

C.-M. Chiang
Department of Chemistry, National SunYat-Sen University, Kaohsiung 804, Taiwan

Introduction

Nanotechnology applications are unlimited in their practical use due to the ability to assemble the nanosized materials to higher ordered and/or functional structures. To realize these great expectations, nanoscientists must deliver truly revolutionary solutions for medical diagnostics (Han et al. 2001; Cheng et al. 2006; Wang et al. 2005), drug delivery (Ferrari 2008; Ferrari 2005), sensors (Kneipp et al. 1999), electronic devices (Tans et al. 1998; Cui and Lieber 2001), or new materials of unique properties (Collier et al. 1998). Importantly, many of these applications are based not on individual nano-objects but rather on assemblies in which these nano-objects interact with one another and organize on purpose. Thus, the challenge that nanoscientists face is to develop efficient and reliable route to assemble nanocomponents.

Self-assembly (Whitesides and Grzybowski 2002; Fialkowski et al. 2006) is probably the most promising candidate for this task. In principle, it can evolve large numbers of individual particles of appropriately chosen properties into higher-order structures. There are several outstanding examples

of successful application of self-assembly at the nanoscale, such as ultrasensitive biosensors (Nam et al. 2003), highly conductive nanowires of uniform-width (Yan et al. 2003), ordered two-dimensional nanoparticle arrays exhibiting unique electronic properties (Murray et al. 2000; Hecht 2005; Dorogi et al. 1995; Shevchenko et al. 2006), as well as the materials of overall macroscopic dimensions and exhibiting unusual bulk properties (Klajn et al. 2007). These demonstrations of nanoscale self-assembly depend crucially on our ability to understand and "engineer" the interactions between nanoparticles and to evolve them into a desired structures.

Self-assembly induced by a verity of methods including solvent evaporation (Pacholski et al. 2002), dedicated procedures involving chemical reactions (Wei et al. 2009), special molecular interactions between the oligonucleotides or biotin–avidin (Mirkin et al. 1996), van der Waals forces (Prasad et al. 2002), electrostatic forces (Kalsin et al. 2006; Maheshwari et al. 2008), dipole–dipole interactions (Tang et al. 2002), organic-bridged ligands (Novak and Feldheim 2000), solvent exchange (Zhang and Wang 2008), with polymer assistance (Kang et al. 2005), and solid phase approaches (Sung et al. 2004) have been shown as the dimeric, trimeric or oligomeric nanostructural assemblies. The self-assembly of the CdTe nanocrystals into nanosheets has achieved by dipole moment, small positive charge and directional hydrophobic attractions (Tang et al. 2006). The peptoid polymers self-assemble into free-floating ultrathin crystalline nanosheets by amphiphilicity, electrostatic recognition, and aromatic interactions were also reported (Nam et al. 2010). Controlling the particle–particle interaction is a major challenge to generate programmable assembly of nanoparticles (Xu et al. 2006) which shows potential usefulness in device fabrication (Feldheim and Keating 1998) and detection systems (Storhoff and Mirkin 1999; Katz and Willner 2004).

Like dipolar interactions, hydrogen bonding is largely electrostatic in nature (Steiner 2002), where a proton mediates the attraction of two larger atoms with partial negative charges. In addition to their widespread use in the superamolecular systems (Lehn 1990; Philp and Stoddart 1996), these molecular interactions have also been applied to self-assembly of larger nanoscale building blocks such as nanoparticles (Boal et al. 2000) and nanorods (Thomas et al. 2004). Magnitudes of individual hydrogen bonding range from 10 to 40 kJ/mol and depend strongly on the solvent conditions (Steiner 2002), where the free energy of hydrogen bond formation is found to be significantly weaker in which molecule–solvent bonds are possible.

At the nanoscale, hydrogen bonding has shown to induce the aggregation of metal nanoparticles functionalized with hydrogen bonding ligands (e.g., $HS–C_6H_4–X$ on gold where X=OH, COOH, NH_2) (Johnson et al. 1998). Degree of aggregation and ordering of the particles depend on the strength of the individual hydrogen bonding formed. For example, very strong hydrogen bonding between divalent hydrogen bonding molecules tethered to Au nanoparticles-induced rapid formation of fibrous nanoparticle gels (Kimura et al. 2004) with characteristic strong, short-ranged potentials. Hydrogen bonding can also be used in a more controlled fashion by site selective functionalization of the particles (Thomas et al. 2004) or by pH responsive hydrogen bonding moieties (Johnson et al. 1998).

Among those derivatives, –COOH-terminated surfaces are of interest for the wide range of applications in surface science (Fisher et al. 2000), electrochemistry (Boubour and Lennox 2000), biology (Groups et al. 2000), sensor development (Bertilsson et al. 1999), and nanoparticles (Auer et al. 2000). An interesting study of the mercaptoacid-induced assembly of Au nanoparticles into chain-like structures was reported by Xia et al. (Cho et al. 2010). They have controlled the self-assemblies of Au nanoparticles into chain-like structures with tunable lengths and interparticular separation by adding $HS(CH_2)_nCOOH$ ($n = 2$, 10, and 15) into a suspension of Au NPs in a mixture of ethanol and water. The number of the Au nanoparticles in the chain-like assemblies could be controlled by adjusting the concentration of the thiols with different alkyl chain. They fixed the structure of these assemblies by coating them with silica shells using the Stöber method or encapsulating them inside gelatin microspheres with a simple fluidic device.

Dimeric assembly of the gold nanoparticles (Sardar et al. 2007) was reported by functionalizing the asymmetrically capped gold nanoparticles with mercaptoacid and mercaptoamine followed by coupling them leads to formation dimers by amide formation between the carboxylic as well as amine group of the surfactants. Not only the homodimers

(16–16 and 30–30 nm) but also heterodimers (41–30, 41–16 and 30–16 nm) were synthesized by this solid phase method.

Fang and coworkers (Fang et al. 2008) have demonstrated a simple method to fabricate an assembled nanostructure from gold nanoparticles. First the individual gold nanoparticles were covered with capping molecules which increase the stability but also to functionalize the particles surface with carboxylic groups. The carboxylic groups were further derived with a linker of Zn^{2+} and derivative nanoparticles were dispersed into buffer solution with different pH to self-assemble the individual nanoparticles into nanostructure.

In this contribution, we present the self-assembly of mercaptoacid (16-MHDA, 11-MUDA and 3-MPA) capped gold nanoclusters (1.8 ± 0.2 nm) into sheets of multilayers. Further study to disturb the self-assembly by the interaction with amines demonstrates that the hydrogen bonding is the responsible factor for the self-assembly. The morphology of the gold clusters was analyzed by TEM, SEM as well as AFM. The luminescent property of the amphiphlic nanoclusters synthesized by this method interestingly depends upon the extent of the surfactant to main alignment of the particles in the sheets.

Experimental section

All preparative operations were carried out under an atmosphere of nitrogen purified by passage through columns of activated BASF catalyst and molecular sieves and using standard Schlenk techniques or in a glove box under N_2. All the chemicals used in this study are commercially available and used without further purification. The precursor (triphenylphosphine)methylgold(I) (CH_3AuPPh_3) was obtained from Strem Chemical Co. The surfactants including 16-mercaptohexadecanoicacid (16-MHDA), 11-mercaptoundecanoicacid (11-MUDA), and 3-mercaptopropionicacid (3-MPA), oleylamine(OAm), 1-octadecylamine (ODAm), 1-hexadecylamine (HDAm), 1-tetradecylamine(TDAm), and 1-octylamine (OctAm) were purchased from ACROS, Aldrich and Fluka Chemical Co. The solvents *o*-xylene, toluene, *n*-hexane, ethanol, and tetrahydrofuran (THF) were purchased from Eco scientific and Co.

Preparation of the mercaptoacid-capped amphiphilic gold nanosheets

The standard procedure for the synthesis of gold nanosheets in organic media is described as following procedure. The precursor CH_3AuPPh_3 (10 mg, 0.0211 mmol) and mercaptoacid (16-MHDA, 11-MUDA, or 3-MPA) (0.0844 mmol) were loaded in a 50-mL three-necked flask equipped with a condenser and a magnetic stir bar in the glove box. After removed from the glove box, the reaction flask was connected to the Schlenk line and filled with N_2. Ten milliliters of *o*-xylene was injected into the reaction flask under nitrogen. The solution mixture was constantly stirred in an oil bath and the temperature of the oil bath was slowly raised to reflux temperature during ca. 1 h. The reaction solution turning to white/pale yellow color indicates the formation of 1.8 ± 0.2 nm gold nanoclusters. The solution was then refluxed for further 3 h to ensure the complete decomposition of the entire precursor. After cooling the solution to room temperature, the nanoproducts were easily isolated by centrifuging the reaction solution at 9,000 rpm for 20 min and drying under vacuum to give white/pale yellow powder. The precipitated Au clusters can be easily re-dispersed in *o*-xylene, toluene, *n*-hexane, THF, ethanol, or deionized water. The effect of the various parameters were examined by altering the conditions such as the precursor/surfactant mole ratio, reaction time, reaction temperature to compare with the standard procedure as mentioned above.

Modified procedures to prepare gold nanobelts

The surfactant solution was first prepared by loading mercaptoacid (0.0844 mmol) and amines (0.0844 mmol) in a in a 50-mL three-necked flask equipped with a condenser and a magnetic stir bar in the glove box. After removed from the glove box, the reaction flask was connected to the Schlenk line and filled with N_2. Five milliliters of *o*-xylene was added into the reaction flask and the solution was refluxed for 1 h under nitrogen atmosphere. The precursor CH_3AuPPh_3 (10 mg, 0.0211 mmol) was loaded in another flask and dissolved in 5 mL of *o*-xylene. The precursor solution was then injected into the reaction flask under nitrogen. The solution mixture was constantly stirred in an oil bath and refluxed for

2 h. The reaction solution turned to white/pale yellow colloidal solution containing the 1.8 ± 0.2 nm Au nanoclusters. After cooling the solution to room temperature, the nanoproducts were easily isolated by centrifuging the reaction solution at 9,000 rpm for 20 min and on drying under vacuum to give white/pale yellow powder.

Characterization of the amphiphilic gold clusters

TEM samples were prepared by dropping few drops of resulting solution on the carbon-coated copper grids (200 mesh) and followed by natural drying. Transmission electron microscopic (TEM) images were recorded on a JEOL JEM-2010 electron microscope at an accelerating voltage of 200 kV. The same samples were used for HR-TEM measurements as well as for electron diffraction analysis. The particle sizes of the samples were measured from TEM images by Sigma Scan-Pro Software. SEM images were recorded on HITACH S-4800 scanning electron microscope. The SEM samples were prepared by adhesion of the dried samples on the carbon film. Fluorescence spectra were recorded at room temperature with HITACHI F-7000 fluorescence spectrophotometer. Powder X-ray diffraction patterns were obtained from Shimadzu XRD-6000 X-ray diffractometer with Cu K_α radiation, $\lambda = 1.5148$ Å. The powder diffraction samples were prepared by adhesion of the Au nanoparticles on the glass substrate. The samples for IR spectral analysis were prepared by squeezing a drop of the reaction solution in $CHCl_3$ solution between the CaF_2 crystals. The prepared liquid film samples were analyzed by JASCO FT/IR-460 spectrometer. ^{13}C NMR spectra of the 16-MHDA as well as 16-MHDA/amine were recorded in Bruker DPK-400 spectrometer. AFM experiments were carried out on a MultiMode atomic force microscope with the NanoScope IIIa controller (Veeco). Si_3N_4 cantilevers were used in all image collection.

Results and discussion

Synthesis of the amphiphilic gold nanoclusters

The amphiphilic nanoclusters were generated by decomposing CH_3AuPPh_3 in *o*-xylene in the presence of mercaptoacid as the capping agents. The standard procedure involves the dissolution of CH_3AuPPh_3 and mercaptoacid (16-MHDA, 11-MHDA, or 3-MPA) (precursor:surfactant mole ratio 1:4) in *o*-xylene under nitrogen atmosphere, raising the solution temperature to 144 °C in 1 h and followed by refluxing the solution for 3 h for the complete decomposition of the precursor. The solution turning to white or pale yellow color indicates the formation of the gold nanoclusters. The decomposition pathway is expected to follow the Eq. 1.

$$2\ CH_3AuPPh_3 \rightarrow\ CH_3 - CH_3 \uparrow + 2\ PPh_3 + 2\ Au^0 \quad (1)$$

Mercaptoacids are well-known examples for the surfactants which induce the self-assembly by formation of hydrogen bonding and lead to chain-like structures. The amphiphilic nature of the mercaptoacids helps to disperse the gold nanoclusters both in the aqueous phase as well as in organic phase. The long hydrocarbon chain acts as a hydrophobic tail, while the easily ionizable –COOH group on the other end is a very good hydrophilic group. Since sulfur atom has the strong affinity towards gold by soft–soft interaction, the thiol group helps to anchor the mercaptoacid molecule on the gold surface while the carboxylic group on the other end of the molecule is responsible for the self-assembly of the clusters to sheets. A representative TEM image of nanosheets composed of Au nanoclusters protected by 16-MHDA is shown in Fig. 1a.

TEM images at various areas showed that more than 95% of the Au nanoclusters self-assembled to give Au nanosheets. High-resolution TEM image of the sheets composed of well aligned Au nanoclusters with the sizes of 1.8 ± 0.2 nm is demonstrated in Fig. 1b. The formation of multilayered sheets is also confirmed by SEM examination (Fig. 1c). The thicknesses of self-assembled Au nanocluster sheets were estimated to be 1.99 nm from AFM examinations (Fig. 1f, g). Dynamic light scattering studies were carried out for the Au cluster sheets dispersed in *n*-hexane and DI water and showed the particle sizes of hundreds of nanometers which indicated the preservation of the self-assembly in the solution phase (supporting information S1). The existence of gold in the nanoclusters is confirmed by EDS (Fig. 1d) and XPS analyses (Fig. 1e). X-ray power diffraction

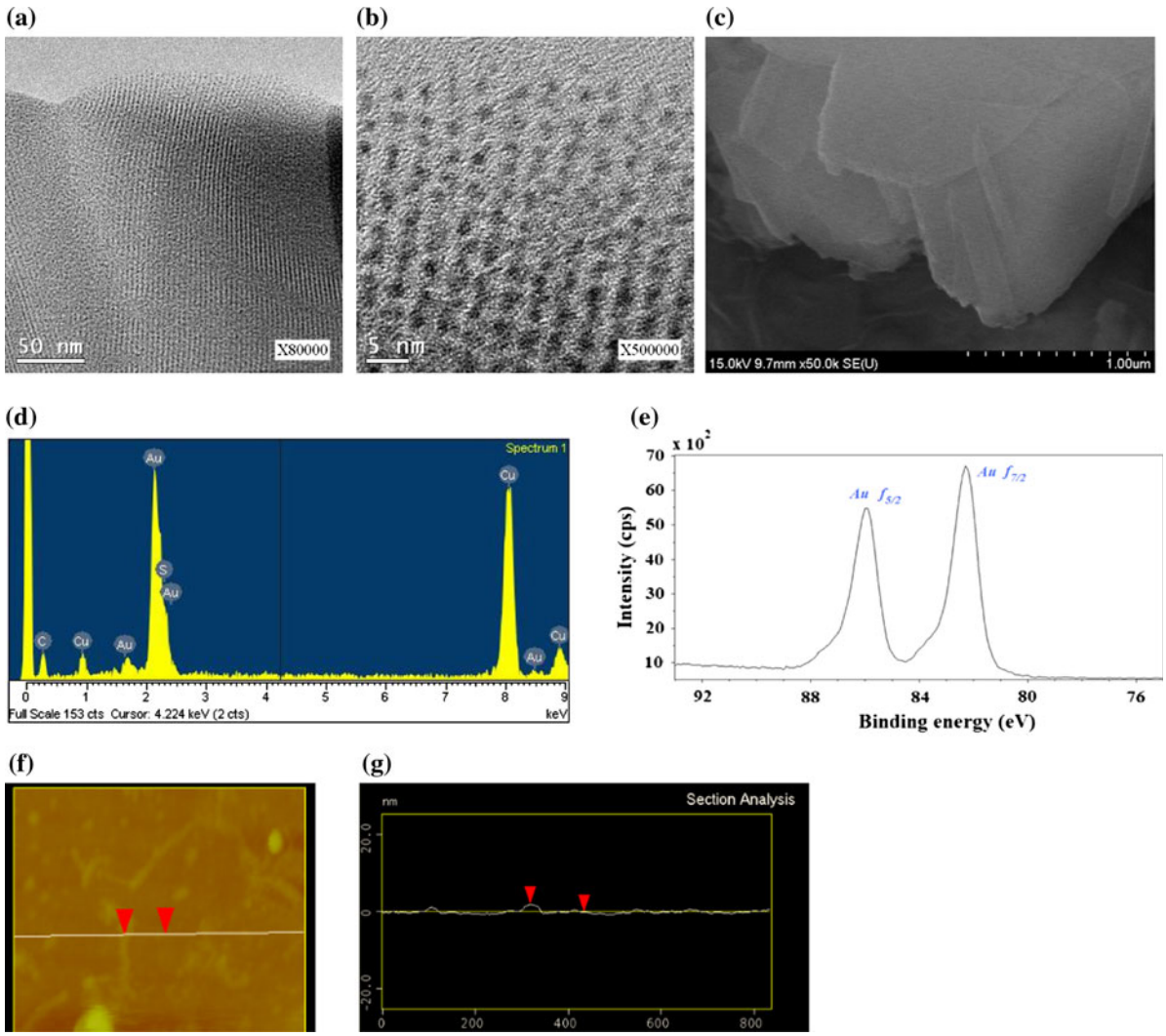

Fig. 1 Characterization of 16-MHDA@ Au nanoclusters prepared in *o*-xylene: **a** TEM image, **b** HRTEM image, **c** SEM image, **d** EDS, **e** XPS data, **f** AFM image, and **g** therespective vertical height profile (monolayer thickness was estimated to be 1.99 nm)

analysis only exhibited very weak diffraction pattern for the nanoclusters sample. The larger gold nanoparticles prepared with lower surfactant loading shows XRD diffraction peaks of (111), (200), and (220) which indicate the fcc structure of the Au nanoclusters (supporting information S2).

The influence of reaction parameters such as carbon chain length of mercaptoacids, precursor to surfactant mole ratio, and reaction time on the formation of the gold nanoparticles was studied by altering these parameters with reference to the standard procedure.

Effect of the mole ratio of precursor:surfactant

Preparation of Au nanoclusturs by decomposition of CH_3AuPPh_3 in the presence of the various amounts of 16-MHDA in *o*-xylene were carried out. TEM images of the gold nanoclusters prepared with different CH_3AuPPh_3:16-MHDA mole ratio are shown in Fig. 2. At the mole ratio of 1:0.5 or below, only larger polydispersed particles were obtained. On further increasing the mole ratio of the surfactant and keeping the amount of precursor constant, the smaller nanoclusters were obtained. It is found that only

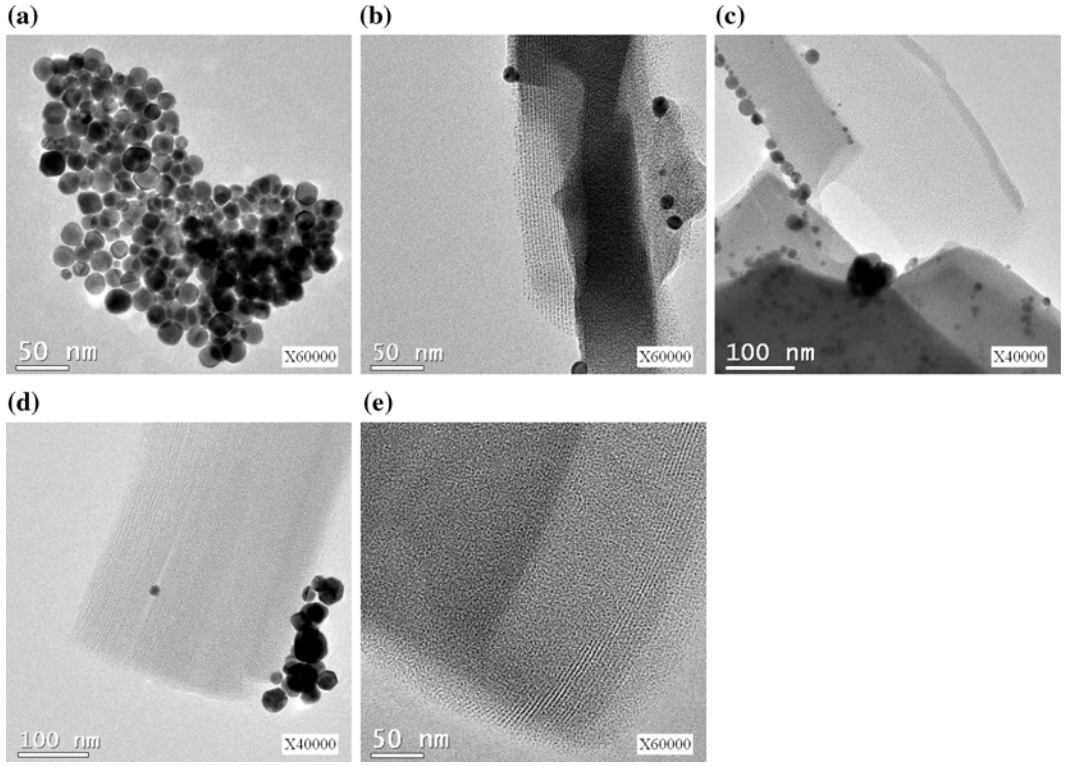

Fig. 2 TEM images of the gold nanocluster sheets prepared with different CH_3AuPPh_3:16-MHDA mole ratio: **a** 1:0.5, **b** 1:1, **c** 1:1.5, **d** 1:2, and **e** 1:4

self-assembled gold clusters (1.8 ± 0.3 nm) exist when the CH_3AuPPh_3:16-MHDA mole ratio reaches 1:4. This observation indicates that four equivalents of the surfactant is the minimum amount required to stabilize the gold nanoclusters, while the surfactants are not sufficient enough to protect the gold nanocluster surface at lower ratios. Similar trends were observed when the nanoparticles were prepared in toluene or with other mercapoacids as capping agents.

Effect of alkyl chain of the surfactant

The effect of the carbon chain length of the mercaptoacids was studied by employing the mercaptoacids with varying number of carbon atoms in the alkyl hydrophobic tail. The reaction was carried out as described in the standard protocol in *o*-xylene. TEM images (Fig. 3) of the gold nanoclusters protected by different mercaptoacid agents revealed their roles in preserving the self-assembly to lead to sheets. The samples with the mercaptoacid having long chains (C16, C11) clearly showed the special type of self-assembly which consists of well aligned particles in the sheets. Though the sheets were formed when the mercaptoacid with shorter chain (C3) was used, no special arrangement of clusters was observed in the sheets. This may be resulted from two reasons. The mercaptoacid with shorter alkyl chain is more hydrophilic and leads to random aggregation the clusters in the sheets in the nonpolar media. Also, the particles capped with shorter carbon chain are more sterically hindered and are prevented to order arrangement.

Effect of reaction time

Examination of the particle morphologies at different reaction times often gives the hint about the mechanism of the formation of the nanoparticles. In order to deduce the mechanism, two different mole ratios were chosen to examine the effect of the reaction time. At precursor to surfactant mole ratio 1:1, the reaction mixture was analyzed soon after raising the

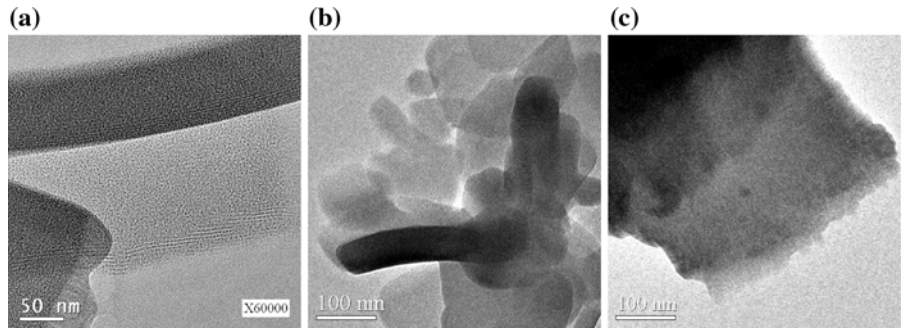

Fig. 3 TEM images of the gold nanocluster sheets with different mercaptoacid surfactants: **a** 16-MHDA, **b** 11-MUDA, and **c** 3-MPA

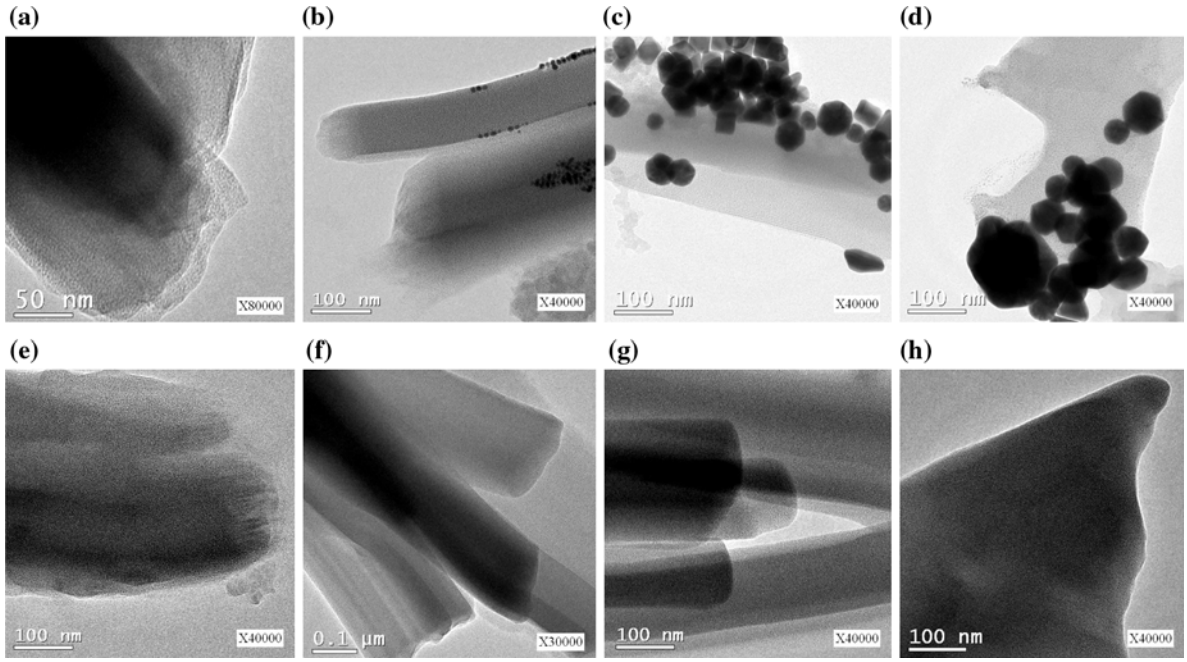

Fig. 4 TEM images of the gold nanoclusters prepared at different reaction times: **a** 0 h, **b** 1 h, **c** 2 h, and **d** 5 h (CH_3AuPPh_3: 16-MHDA = 1:1); **e** 0 h, **f** 1 h, **g** 2 h, and **h** 5 h (CH_3AuPPh_3:16-MHDA = 1:4)

temperature to reflux and well assembled gold clusters with the size 1.8 ± 0.2 nm were observed (Fig. 4a). Further refluxing the reaction solution for 5 h, the larger particles were formed in addition to the nanoclusters (Fig. 4b–d). While at precursor to surfactant mole ratio 1:4, only self-assembled nanoclusters were observed throughout the reaction for 5 h (Fig. 4e–f). This observation clearly shows the importance of the amount of the surfactant in order to stabilize the self-assembled cluster sheet. The formation of clusters is a dominant process in the initial stage of the reaction at lower temperatures, and further refluxing the reaction solution facilitates the growth of the particles if they are not sufficiently protected by the mercaptoacids. Whereas well-protected nanoclusters preserve its morphology even the reaction time is extended.

Mercaptoacid-induced self-assembly of the amphiphilic cluster sheets

As described in previous section, TEM and SEM images of the samples prepared (16-MHDA as surfactant) according to the standard procedure revealed the presence of Au nanosheets which are composed of aligned nanoparticles. It is believed that

Scheme 1 Schematic plot to demonstrate the self-assembly of Au nanoparticles to nanosheets

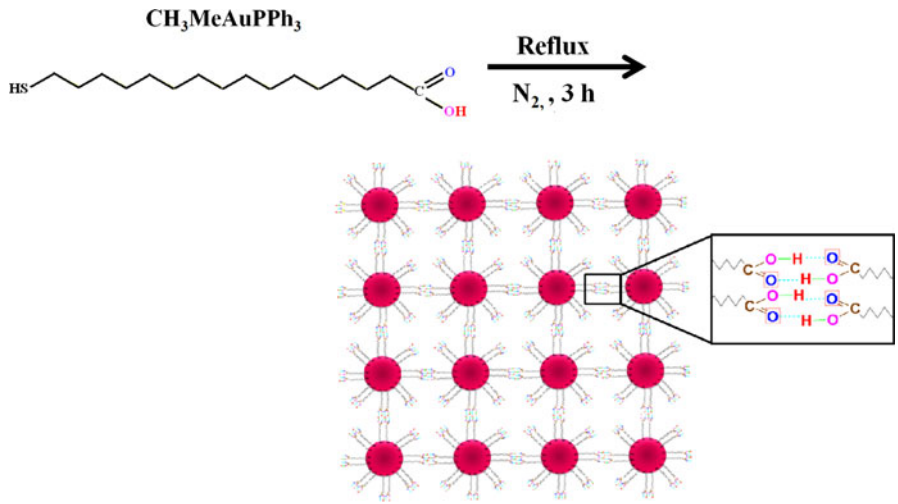

the hydrogen bonding between the carboxylic groups resulted in the formation of the nanosheets demonstrated as Scheme 1.

The preliminary investigation was carried out by recording the IR spectra of the liquid samples of the cluster sheets as well as the surfactant (16-MHDA). The CO stretching peaks were observed for both the sample (1,699 cm^{-1}) and 16-MHDA (1,698 cm^{-1}) which correspond to the hydrogen-bonded carbonyl group (supporting information S3). In addition, a very broad OH stretching band at $\sim$3,000 cm^{-1} is responsible for the intermolecular hydrogen-bonded hydroxyl group. The effect of the solvents on the self-assembly is explored by dispersion of the gold clusters prepared in several solvents with different polarity and followed by examination of their morphologies from TEM images (Fig. 5). The observation of the similar self-assembly of 16-MHDA-capped gold nanoclusters in various solvents indicates the hydrogen boding between the carboxylic groups of the surfactants is strong enough not to be affected by the highly polar solvents like DI water and ethanol (Fig. 5d, e).

Addition of amines to interrupt the hydrogen bonding between the self-assembled clusters

In order to interrupt the hydrogen bonding between the carboxylic groups of surfactant molecules on the adjacent clusters, a slightly modified procedure involving the addition of amines with mercaptoacid in the standard procedure was carried out. Decomposition of CH_3AuPPh_3 in the presence of preheated mixture of 16-MHDA and amine (ODAm, HDAm, TDAm, ODAm, Oct.Am) in *o*-xylene gave the products of gold nanobelts whose TEM images are shown in Fig. 6. In all cases the nanosheets of few tens of nanometers were observed. The similar experiments by using other combinations of mercaptoacid and alkylamine also led to the similar results (supporting information S4).

The reduction in the size of the Au nanocluster self-assemblies from nanosheets to nanobelts is likely due to part of the carboxylic groups of the mercaptoacid coupling with amine to form NH_3^+–$^-$OOC pair and blocking of hydrogen bonding sites. This is confirmed by comparing the carbonyl region in ^{13}C spectra of the 16-MHDA and refluxed mixture of ODAm and 16-MHDA. Only one peak was observed at 180.3 ppm for the carbonyl carbon of the carboxylic acid group in case of 16-MHDA. For the mixture of ODAm and 16-MHDA sample, two different carbonyl peaks were observed at 180.12 and 159.59 ppm assigned for the carbon of the carboxylic acid and carboxylate anion, respectively (supporting information S5)

In order to examine the stability of the self-assembled gold nanosheets, the 16-MHDA-capped Au nanosheets was mixed with ODAm in *o*-xylene and the mixture was refluxed for 2 h. The gold nanosheets remained intact in the solution (supporting information S6). This observation clearly indicates the strong hydrogen bonding between the carboxylic groups of the mercaptoacid molecules is strong enough to prevent the attack of alkylamine

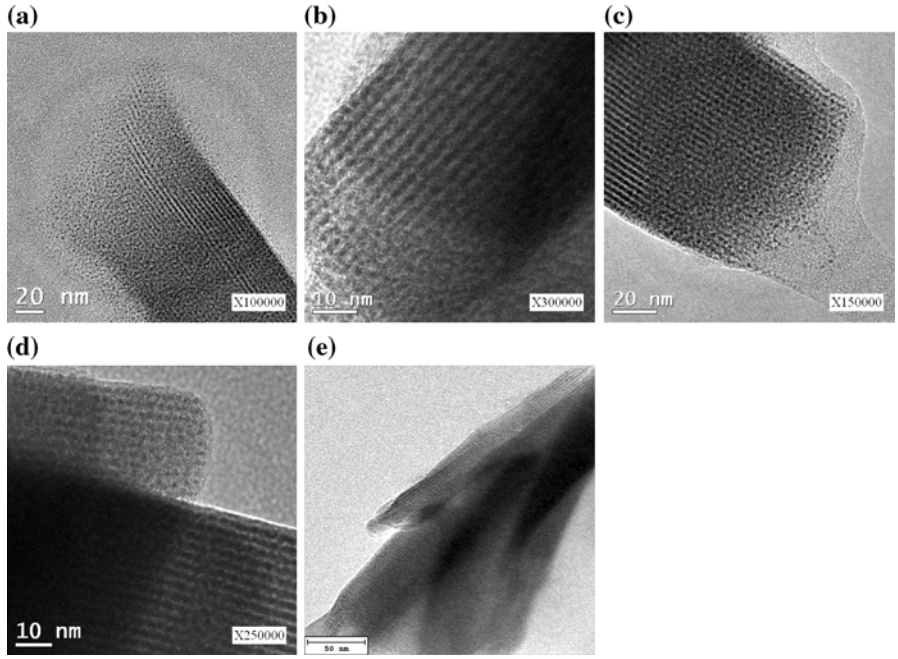

Fig. 5 TEM images of 16-MHDA@Au nanocluster sheets dispersed in different solvents: **a** *n*-hexane, **b** *o*-xylene, **c** THF, **d** DI water, and **e** ethanol

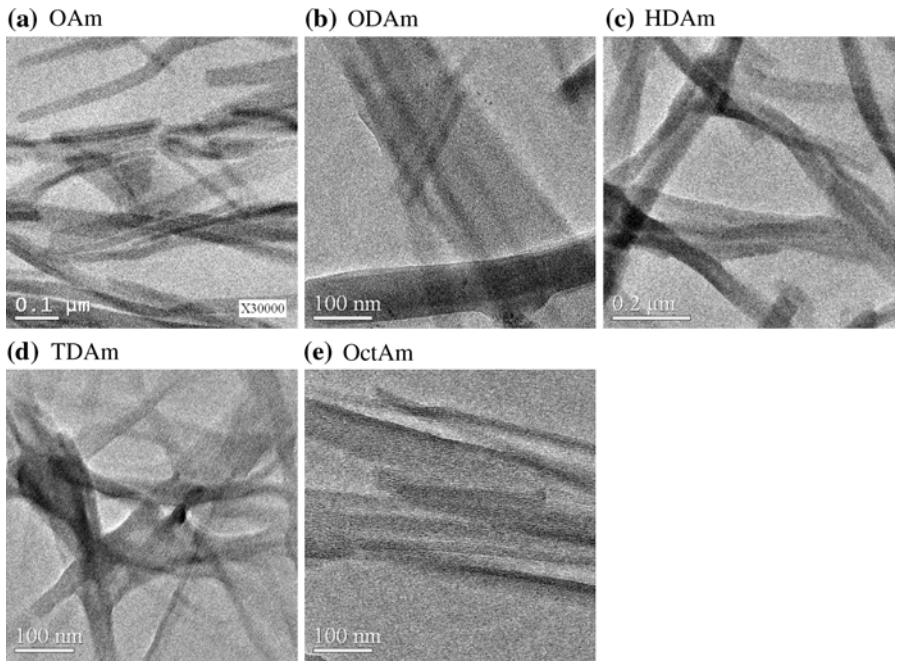

Fig. 6 TEM images of the gold nanocluster sheets prepared in presence of 16-MHDA and various amines **a** OAm, **b** ODAm, **c** HDAm, **d** TDAm, and **e** OctAm

and provides high stability of gold nanosheets. Pre-reflux of 16-MHDA and ODAm is a crucial step to block the intermolecular hydrogen bonding of mercaptoacids and to disturb the self-assembly of Au nanoclusters.

Luminescent properties of the gold cluster sheets

Optical properties of ampiphilic gold clusters were investigated by UV–vis absorption as well as photoluminescence (PL) spectroscopic analysis. Interestingly,

the luminescent properties of gold nanoclusters depend on the amount of the mercaptoacid loaded on the gold particle surface. The luminescence spectra were recorded by exciting the samples at 330 nm. A single PL peak located between 500 and 700 nm and the intensity decreases with increasing the amount of the surfactant on the particle surface. Figure 7 represents the Au nanoclusters prepared with different precursor:surfactant mole ratio. At lower ratios (1:0.5 and 1:1), less intense band is due to the presence of great amount of the larger particles rather than clusters. The luminescence intensity increases with the ratio increasing up to 1:2 because of the existence of larger proportions of smaller clusters. Further increasing the ratio leads to disappearance of the luminescent band because of the self-assembly of the nanoclusters to form the nanosheets. This result is consistent with TEM images shown in Fig. 1.

Similar observation is observed for the 16-MHDA-amine protected particles prepared by the modified procedure. Figure 8 shows the effect of various amounts of HDAm with the fixed amount of the 16-MHDA-capped gold clusters. The Au clusters protected with 16-MHDA:HDAm mole ratio 4:2–4:6 shows the intense luminescence. When the mole ratio amine is raised further to 4:8, it leads to the absence of luminescence band. This may be due to the destabilization of the regular assembly of the clusters in the presence of excess amine leads to the random aggregation of the clusters (supporting information S7). With amines of varying polarity, OctAm showed intense band where as the OAm showed the least

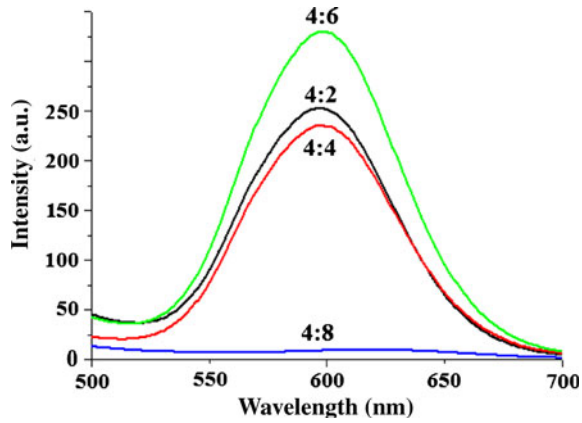

Fig. 8 Luminescent spectra of gold clusters prepared at different 16-MHDA:HDAm mole ratios

intense luminescent band (Fig. 9). It is known that the shorter the amine more polar in nature which had much more tendency to form ion pair with –COOH group. Hence compare to the long chain amine the sample with the shorter C8 amine combine with more number of carboxylic groups attached on the gold surface and convert them carboxylate-ammonium ion pair surfactant system intern increase the tendency of the clusters to be separated leads to intense luminescent band. Similar trend is observed for the 11-MUDA/various amines. In all the samples PL is stronger when excited between 310 and 360 nm and very weak when excited below 300 nm and more than 380 nm. On comparing the larger intensity of the total luminescent to less intense fluorescent spectral band as well as the observation of the stroke shift between excitation and emission energies for all

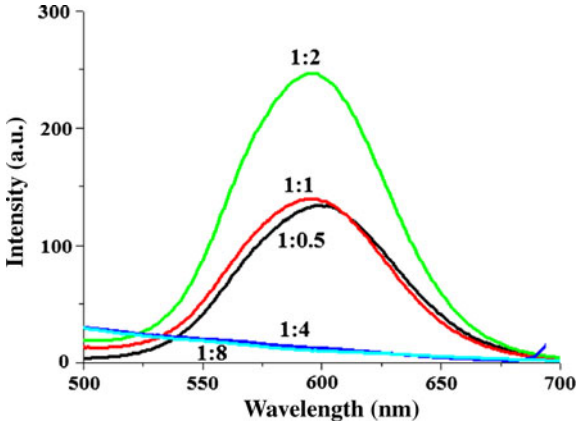

Fig. 7 Luminescent spectra of amphiphilic gold clusters prepared at different $MeAuPPh_3$:16-MHDA mole ratios

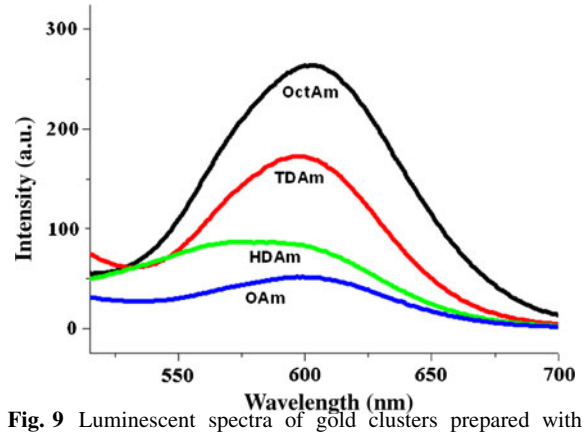

Fig. 9 Luminescent spectra of gold clusters prepared with 16-MHDA and different

samples point outs the phosphorescence nature of their emission similar to the previously reported gold(I)-alkanethiolate complexes.

Conclusion

In summary, self-assembly of the amphiphilic clusters into monolayered sheets were demonstrated by capping the Au nanoclusters ($\sim$2 nm) with mercaptoacids. The aurophilic mercapto group anchors the mercaptoacid molecules on the gold surface, while the carboxylic acid group of mercaptoacid molecules attached on the adjacent gold cluster surface to form the hydrogen bonding between them and drives the self-assembly process. The change in morphology of the sheets by interaction with amines confirms the interaction between the carboxylic acid groups and leads to the formation of the carboxylate-ammonium ion pair to reduce the hydrogen bonding terminus. Interestingly, we found the dependency of the luminescent properties on the extent of maintaining the self-assembly of the clusters by stabilizing them from random aggregation intern dictated by the surfactants.

Acknowledgments We are grateful to the National Science Council of the Republic of China for the financial support (NSC97-2113-M-194-009-MY2) and The Instrumental Centers in National Chung Cheng University for the TEM, SEM, EDX, and electron diffraction analyses.

References

Auer F, Scotti M, Ulman A, Jordan R, Sellergren B, Garno J, Liu GY (2000) Nanocomposites by electrostatic interactions: 1 Impact of sublayer quality on the organization of functionalized nanoparticles on charged self-assembled layers. Langmuir 16:7554–7557

Bertilsson L, Potje-Kamloth K, Liess HD, Liedberg B (1999) On the adsorption of dimethyl methylphosphonate on self-assembled alkanethiolate monolayers: influence of humidity. Langmuir 15:1128–1135

Boal AK, Ilhan F, DeRouchey JE, Thurn-Albrecht T, Russell TP, Rotello VM (2000) Self-assembly of nanoparticles into structured spherical and network aggregates. Nature 404:746–748

Boubour E, Lennox RB (2000) Insulating properties of self-assembled monolayers, monitored by impedance spectroscopy. Langmuir 16:4222–4228

Cheng MMC, Cuda G, Bunimovich YL, Gaspari M, Heath JR, Hill HD, Mirkin CA, Nijdam AJ, Terracciano R, Thundat T, Ferrari F (2006) Nanotechnologies for biomolecular detection and medical diagnostics. Curr Opin Chem Biol 10:11–19

Cho EC, Choi SW, Camargo PHC, Xia Y (2010) Thiol-induced assembly of Au nanoparticles into chainlike structures and their fixing by encapsulation in silica shells or gelatin microspheres. Langmuir 26:10005–10012

Collier CP, Vossmeyer T, Heath JR (1998) Nanocrystal superlattices. Annu Rev Phys Chem 49:371–404

Cui Y, Lieber CM (2001) Functional nanoscale electronic devices assembled using silicon nanowire building blocks. Science 291:851–853

Dorogi M, Gomez J, Osifchin R, Andres RP, Reifenberger R (1995) Room-temperature coulomb blockade from a self-assembled molecular nanostructure. Phys Rev B 52: 9071–9077

Fang C, Fan Y, Kong JM, Gao ZQ, Balasubramanian N (2008) Preparation of nanochain and nanosphere by self-assembly of gold nanoparticles. Appl Phys Lett 92:263108-1–263108-3

Feldheim DL, Keating CD (1998) Self-assembly of single electron ttransistors and related devices. Chem Soc Rev 27:1–12

Ferrari M (2005) Cancer nanotechnology: opportunities and challenges. Nat Rev Cancer 5:161–171

Ferrari M (2008) Beyond drug delivery. Nat Nanotechnol 3: 131–132

Fialkowski M, Bishop KJM, Klajn R, Smoukov SK, Campbell CJ, Grzybowski BA (2006) Principles and implementations of dissipative (dynamic) self-assembly. J Phys Chem B 110:2482–2496

Fisher GL, Hooper AE, Opila RL, Allara DL, Winograd N (2000) The interaction of vapor-deposited Al atoms with CO_2H groups at the surface of a self-assembled alkanethiolate monolayer on gold. J Phys Chem B 104: 3267–3273

Groups A, Chapman RG, Ostuni E, Yan L, Whitesides GM (2000) Preparation of mixed self- assembled monolayers (SAMs) that resist adsorption of proteins using the reaction of amines with a SAM that presents interchain carboxylic. Langmuir 16:6927–6936

Han M, Gao X, Su JZ, Nie S (2001) Quantum-dot-tagged microbeads for multiplexed optical coding of biomolecules. Nat Biotechnol 19:631–635

Hecht S (2005) Optical switching of hierarchical self-assembly: towards "enlightened" materials. Small 1:26–29

Johnson SR, Evans SD, Brydson R (1998) Influence of a terminal functionality on the physical properties of surfactant-stabilized gold nanoparticles. Langmuir 14:6639–6647

Kalsin AM, Fialkowski M, Paszewski M, Smoukov SK, Bishop KJM, Grzybowski BA (2006) Electrostatic self-assembly of binary nanoparticle crystals with a diamond-like lattice. Science 312:420–424

Kang Y, Erickson KJ, Taton TA (2005) Plasmonic nanoparticle chains via a morphological, sphere-to-string transition. J Am Chem Soc 127:13800–13801

Katz E, Willner I (2004) Integrated nanoparticle–biomolecule hybrid systems: synthesis, properties, and applications. Angew Chem Int Ed 43:6042–6108

Kimura M, Kobayashi S, Kuroda T, Hanabusa K, Shirai H (2004) Assembly of gold nanoparticles into fibrous

aggregates using thiol-terminated gelators. Adv Mater 16:335–338

Klajn R, Bishop KJM, Fialkowski M, Paszewski M, Campbell CJ, Gray TP, Grzybowski BA (2007) Plastic and moldable metals by self-assembly of sticky nanoparticle aggregates. Science 316:261–264

Kneipp K, Kneipp H, Itzkan I, Dasari RR, Feld MS (1999) Ultrasensitive chemical analysis by Raman spectroscopy. Chem Rev 99:2957–2975

Lehn JM (1990) Perspectives in supramolecular chemistry—from molecular recognition towards molecular information processing and self-organization. Angew Chem Int Ed 29:1304–1319

Maheshwari V, Kane J, Saraf RF (2008) Self-assembly of a micrometers-long one-dimensional network of cemented Au nanoparticles. Adv Mater 20:284–287

Mirkin CA, Retsinger RL, Mucic RC, Storhoff J (1996) A DNA-based method for rationally assembling nanoparticles into macroscopic materials. Nature 382:607–609

Murray CB, Kagan CR, Bawendi MG (2000) Synthesis and characterization of monodisperse nanocrystals and close-packed nanocrystal assemblies. Annu Rev Mater Sci 30:545–610

Nam J-MC, Thaxton S, Mirkin CA (2003) Nanoparticle-based bio-bar codes for the ultrasensitive detection of proteins. Science 301:1884–1886

Nam KT, Shelby SA, Choi PH, Marciel AB, Ritchie R, Tan L, Chu TK, Mesch RA, Lee B-C, Connolly MD, Kisielowski C, Zuckermann RN (2010) Free-floating ultrathin two-dimensional crystals from sequence-specific peptoid polymers. Nat Mater 9:454–460

Novak JP, Feldheim DL (2000) Assembly of phenylacetylene-bridged silver and gold nanoparticle arrays. J Am Chem Soc 122:3979–3980

Pacholski C, Kornowski A, Weller H (2002) Self-assembly of ZnO: from nanodots to nanorods. Angew Chem Int Ed 41:1188–1191

Philp D, Stoddart JF (1996) Self-assembly in natural and unnatural systems. Angew Chem Int Ed 35:1154–1196

Prasad BLV, Stoeva SI, Sorensen CM, Klabunde KJ (2002) Digestive ripening of thiolated gold nanoparticles: the effect of alkyl chain length. Langmuir 18:7515–7520

Sardar R, Heap TB, Shumaker-Parry JS (2007) Solid phase synthesis of gold nanoparticle dimers using and asymmetric functionalization approach. J Am Chem Soc 129:5356–5357

Shevchenko EV, Talapin DV, Kotov NA, O'Brien S, Murray CB (2006) Structural diversity in binary nanoparticles superlattices. Nature 439:55–59

Steiner T (2002) The hydrogen bond in the solid state. Angew Chem Int Ed 41:48–76

Storhoff JJ, Mirkin CA (1999) Programmed materials synthesis with DNA. Chem Rev 99:1849–1862

Sung K-M, Mosley DW, Peelle BR, Zhang S, Jacobson JM (2004) Synthesis of monofunctionalized gold nanoparticles by Fmoc solid-phase reactions. J Am Chem Soc 126:5064–5065

Tang Z, Kotov NA, Giersig M (2002) Spontaneous organization of single CdTe nanoparticles into luminescent nanowires. Science 297:237–240

Tang Z, Zhang Z, Wang Y, Glotzer SC, Kotov NA (2006) Self-assembly of CdTe nanocrystals into free-floating sheets. Science 314:274–278

Tans SJ, Verschueren ARM, Dekker C (1998) Room-temperature transistor based on a single carbon nanotube. Nature 393:49–52

Thomas KG, Barazzouk S, Ipe BI, Joseph STS, Kamat PV (2004) Uniaxial plasmon coupling through longitudinal self-assembly of gold nanorods. J Phys Chem B 108: 13066–13068

Wang Z, Lee J, Cossins AR, Brust M (2005) Microarray-based detection of protein binding and functionality by gold nanoparticle probes. Anal Chem 77:5770–5774

Wei Y, Bishop KJM, Kim J, Soh S, Grzybowski BA (2009) Making use of bond strength and steric hindrance in nanoscale "synthesis". Angew Chem Int Ed 48:9477–9480

Whitesides GM, Grzybowski B (2002) Self-assembly at all scales. Science 295:2418–2421

Xu X, Rosi NL, Wang Y, Huo F, Mirkin CA (2006) Asymmetric functionalization of gold nanoparticles with oligonucleotides. J Am Chem Soc 128:9286–9287

Yan H, Park SH, Finkelstein G, Reif JH, LaBean TH (2003) DNA-templated self-assembly of protein arrays and highly conductive nanowires. Science 301:1882–1884

Zhang H, Wang D (2008) Controlling the growth of charged-nanoparticle chains through interparticle electrostatic repulsion. Angew Chem Int Ed 47:3984–3987